FABRICATION AND NANOMECHANICAL TESTING OF CONDUCTIVE NANOCOMPOSITE FILAMENTS FOR FFF 3D PRINTING: DEVELOPMENT OF A 3D PRINTED EMERGENCY STOP BUTTON

Evangelos Meretis[1], Emmanouil K. Tzimtzimis[1], Konstantinos Tsongas[1], Panagiotis Kyratsis[2] Dimitrios Tzetzis[1*]

[1]Digital Manufacturing and Materials Characterization Laboratory, School of Science and Technology, International Hellenic University, 57001 Thessaloniki, Greece

[2] University of Western Macedonia, Department of Product and Systems Design Engineering, Kila Kozani,50100, Greece

**Corresponding author: Dimitrios Tzetzis, d.tzetzis@ihu.edu.gr.*

***ABSTRACT**: 3D printing is an innovative and unique additive manufacturing technology that offers a high degree of freedom for the creation of various products including electrical parts, such as sensors, switches and connectors. The ease of access in low-cost, dependable, conductive material will be vital in the fabrication of these products. Nowadays there are not many reliable 3D printable conductive filament composites with adequate conductive properties that can be used in the fabricate circuits using the fused filament fabrication (FFF) method. In view of this, the current paper presents the fabrication, testing, characterization and application of an inexpensive thermoplastic conductive material that has been formed into filament form for 3D printing. Results from the dynamic ultra-micro-hardness tests, as well as SEM analysis are thoroughly presented in order to fully define the mechanical properties of the developed composites necessary for conductive structural parts. An emergency stop button (e-stop) was designed and 3D printed with the newly created prototype and applied to a small circuit design in order to demonstrate the potential use of such composites into circuit applications.*

***KEYWORDS**: Additive manufacturing, Thermoplastic conductive composite, 3D printing*

1 INTRODUCTION

3D printing is an innovative additive manufacturing technology that offers a high degree of freedom for the creation of various customized products (Cephas, 2014). In the modern era of technology, the plethora of efficient, reliable 3D printers has made this unique technology an increasingly low-cost, viable option for manufacturing customized products. Several companies have taken advantage of additive manufacturing tools for prototyping various products and parts such as flexible and stretchable sensors, antennas, industrial scale parts, as an example in the power industry for producing turboexpanders for decentralized micro-power systems (Novotny et al., 2018) and in various electronic sensors (Marasso et al, 2018). The electrically conductive materials embedded into these products are using carbon-based, metal-ion or colloid conductive composite inks. Even though, metal-ion or -colloid ink such as silver ion or silver nanoparticles have a higher conductivity-lower electrical resistivity than carbon-based composites (Horst and Junior, 2019), carbon-based polymer materials achieve two great advantages for 3D-printed electronics. The first and most significant one is the absence of additional processing in carbon-based polymer composites such as thermal annealing or evaporation of solvent, which are required by 3D printing with the metal-ion composites. And secondly, they can be easily manufactured into a filament form for FFF printing. This procedure motivates home users to fabricate conductive 3D printed parts utilizing inexpensive desktop 3D printers.

Carbon black is manufactured by the incomplete combustion of heavy petroleum products such as Fluid Catalytic Cracking (FCC) tar, coal tar, or ethylene cracking tar. Carbon black is a kind of paracrystalline carbon with a high surface-area compared to each volume ratio, even though lower compared to activated carbon (Horst and Junior, 2019). The microstructure of carbon black is related to graphite, while the layers are not structured with the same order, especially toward the core of the particle. Therefore, carbon black is an fundamental semiconductor. The level of influence of carbon black an electrically resistive polymer to become conductive is dependent on the physical and

chemical properties of the carbon black (Wei et al, 2015), (Moore, 1973).

On the other hand, owing to the material's exceptional stiffness and strength, carbon nanotubes (CNTs) are fabricated with an aspect ratio of up to 132,000,000:1, considerably greater than that for any other material. Moreover, due to their remarkable thermal conductivity and electrical, along with their mechanical properties, carbon nanotubes may find applications as additives to various structural matrix materials (Suder et al, 2016), (Assael et al, 2009), (Mansour et al 2017), (Tsongas et al, 2017). (Klonos et al, 2019). Consequently, CNTs are considered as ideal candidates for thermoelectric power generation, since there is a constant scientific concern to improve the electrical conductivity, the Seebeck coefficient and power factor values. Therefore, CNTs were chosen as the second conductive filler along with carbon black for the project.

The current paper describes the preparation, characterization and 3D-printing application of low-cost thermoplastic composite filaments based on Acrylonitrile Butadiene Styrene (ABS) as polymeric matrix. The conductive filler that is used in order to produce the conductive filament is carbon black (CB) along with carbon nanotubes. To evaluate the performance of the filaments fabricated with the proposed materials a dynamic ultra-micro-hardness tester was utilized in order to fully define properties such as hardness and elastic modulus. The structure of the filament was characterized with scanning electron microscopy. Following filament fabrication and selection a 3D printing case study is presented by using the conductive filaments as structural materials. Therefore, an emergency stop button (e-stop) prototype was designed and printed with an FFF 3D printer, using a selected prototype conductive filament and applied to a small circuit design in order to demonstrate the potential use of such approach to applications requiring circuitry.

2 MATERIALS AND METHODS

2.1 Preparation of conductive thermoplastic composites

The conductive composite was prepared by the solution mixing method and particularly by mixing ABS pellets along with carbon black powder, CNTs, Triethyl Citrate (TEC) and acetone. Three prototype material categories utilizing ABS as a matrix element were created. The first category was ABS loaded with conductive paint (Bare Conductive, London UK) in various percentages, the second category of prototype material was ABS loaded with carbon black powder (Vellis Chemicals, Thessaloniki, Greece) in various percentages and lastly the third category was ABS loaded with carbon black powder and carbon nanotubes (OCSiAl, Luxenburg, Luxenburg) in various percentages. In total, seven types of samples have been fabricated. Samples of commercial ABS filament were used for reference purposes. ABS/Cpaint30% filament composed of 70% ABS and 30% Conductive paint. ABS/CB30% samples composed of 70% ABS and 30% Carbon Black were tested as filament and were 3D printed. Also, ABS/CB15% samples composed of 85% ABS and 15% Carbon Black were tested in a filament form. ABS/2%CNTs/CB15% samples composed of 78% ABS, 15% Carbon Black, 2% CNTs and 5% TEC plasticizer and they were tested as filament while they were 3D printed as well. By consecutively adding the aforementioned materials into an acetone mixture and applying an ultrasonic sonication, a homogenous liquid was created. Ultrasonic sonication (UP200S, Hielscher, Teltow, Germany) improves dispersion, uniformity and stability of particles. The aforementioned benefits cannot be obtained with magnetic stirrers (Vieira et al, 2011). In the second step of the procedure an oven (FD 56, Binder GmbH) was used in order to evaporate all of the acetone and humidity from the solution. Humidity in some cases is the cause of nozzle blockage on the liquefier of the FFF printing machine (Teanmetawong et al, 2019). That procedure led to the production of a solid material, which was then imported into a rapid shredder in order to create pellets.

2.2 Fabrication of 3D printable conductive filament

The final material shaped into filament form was created by processing the pellets with a single screw extruder (Filabot Extruder, Filabot) with a 3mm nozzle. Pelletizing the composite (Bosch Rapid Shredder AXT 2200, Gerlingen, Germany) was a crucial procedure in order to create a homogenous filament form composite (Halidi et al, 2012). All the samples and the e-stop button were designed in Solidworks (Dassault Systemes, France) and 3D-printed with BCN3D Sigma R17 3D (BCN3D, Barcelona, Spain) printer using Cura (Ultimaker, Utrecht, Netherlands) slicing software. The e-stop button was 3D printed with ABS filament and composite filament with a printing resolution of 100μm and 20% grid infill pattern. Finally, the extruder and the heated bed temperatures were 205°C and 65°C, respectively.

2.3 Microstructure characterization

The morphology of the samples was examined using scanning electron microscopy (Phenom ProX, ThermoFischer, Netherlands). The samples were

mounted onto double adhesive conductive carbon tabs (TED Pella, Redding, CA, USA) on an aluminum stub and were carbon-coated using an ion sputtering device (Quorum SC7620, East Sussex, UK).

2.4 Nanoindentation testing

Analysis of the mechanical properties of the compounds in a filament and printed forms were performed using a dynamic ultra-micro-hardness tester (DUH-21S; Shimadzu Co., Kyoto, Japan), which was fitted with a 100 nm radius triangular pyramidal tip (Berkovich – type indenter). Such tests precisely measure the local variations of elastic modulus and hardness (Tzetzis et al, 2017), (Tsongas et al, 2019), (Mansour et al, 2013,2021), (Mansour and Tzetzis 2013). From the instrumented indentation tests the load of the indenter is recorded as a function of the indentation depth. The dynamic micro-indentation test was carried out with peak loads of 500 mN for the filament form samples and 100 mN for the 3D printed samples. The load rate was remained constant at 13.324 mN/s, and the hold time at the maximum load was set to 3s. The dynamic micro-indentation results, such as indentation hardness and elastic modulus, were calculated as the average values of five measurements.

The indentation hardness and modulus values of the nanocomposite filament and 3D printed specimens were determined based on the calculation method of Oliver and Pharr (Oliver and Pharr, 1992). The hardness can be calculated as a function of the maximum penetration depth of the indentation:

$$H=\frac{P_{max}}{A} \quad (1)$$

where P_{max} is the maximum applied load measured at the maximum depth of penetration (h_{max}) and A is the projected contact area between the indenter and the film. For a perfect Berkovich indenter, A can be expressed as a function of the contact indentation depth h_f as:

$$A=3\sqrt{3}h_f^2\tan^2 65=23.96h_f^2 \quad (2)$$

The contact indentation, h_f, can be determined from the following expression:

$$h_f=h_{max}-\varepsilon\frac{P_{max}}{S} \quad (3)$$

where ε is a geometric constant ε=0.75 for a pyramidal indenter and S is the contact stiffness that can be determined as the slope of the unloading curve at the maximum loading point, i.e.

$$S=\left(\frac{dP}{dh}\right)_{h=h_{max}} \quad (4)$$

The reduced elastic modulus E_r is given by:

$$E_r=\frac{S}{2\beta}\sqrt{\frac{\pi}{A}} \quad (5)$$

where β is a constant that depends on the geometry of the indenter. For the applied Berkovich indenter the parameter β was equal to 1.034. The specimen elastic modulus (E_s) can then be calculated as:

$$\frac{1}{E_r}=\frac{1-\upsilon_s^2}{E_s}+\frac{1-\upsilon_i^2}{E_i} \quad (6)$$

where $E_{i,s}$, and $\nu_{i,s}$ are the elastic modulus and the Poisson's ratio for the indenter and the specimen, respectively. Moreover, for a diamond indenter, E_i is 1140 GPa and ν_i is 0.07. The specimen's hardness H and elastic modulus E_s were computed from the set of equations documented above

3 RESULTS AND DISCUSSION

3.1 Mechanical behavior

The 3D printed object should have sufficient mechanical strength and stiffness to ensure the durability of the end-product for the specific application. In total, seven samples were created in order to fully obtain mechanical properties with the Dynamic Micro-Indentation Test. The typical nanoindentation load–depth curves of the ABS composite filaments are displayed in Figure 1.

Table 1 presents the total deformation (ht) values, which are the sum of plastic deformation (hp) and elastic deformation (he), of the seven samples under study. The indentation deformation, ht = hp + he, is always satisfied. The hp/ht and he/ht ratios are also listed, along with the standard deviation of ht, hp and he. The filament ABS/2%CNTs/CB15% showed significantly larger ht and hp values than the other composites, while the ABS/2%CNTs/CB15% also had a high hp/ht ratio. On the contrary, the ABS/ CB 30% and ABS/2%CNTs/CB15% materials, which are the only two printed material samples measured, showed significantly smaller ht and hp values than the other composites. These two samples also had a ratio of hp/ht and he/ht similar to the reference ABS sample.

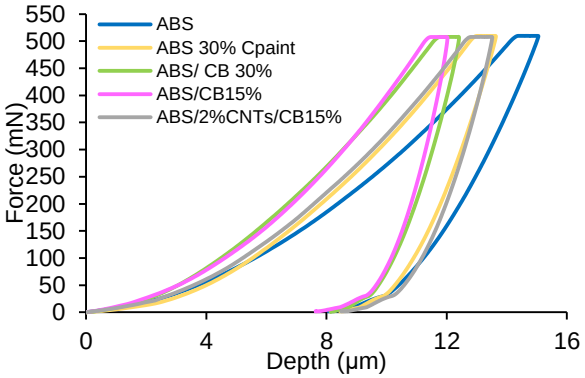

Fig. 1 Typical force-nanoindentation depth curves of ABS composite filaments

In addition, Table 2 summarizes the hardness values and elastic moduli of the samples. The bar charts along with the error bar are demonstrated in Figure 2. The hardness of the composites ranged from 127.26 to 181.42 MPa with ABS/CB15% Filament demonstrating the highest value. The elastic moduli of the composites ranged from 1847.33 to 3660.33 MPa. Again ABS/CB15% showed the highest elastic modulus among all the samples. All the composite specimens exhibited both higher hardness and higher elastic modulus compared to the reference ABS sample. As shown in Figure 2, adding 30% conductive paint in the reference ABS sample, increased the elastic modulus and the hardness by 37% and 13% respectively. Also, adding 15% Carbon Black (filament form), 30% (filament form) and 30% (Printed form) in the reference ABS sample, resulted in increasing the elastic moduli by 91%, 98% and 16% respectively. In addition, the carbon black fillers resulted in the increase of the hardness by 22%, 42% and 42% respectively.

Table 1 Total, plastic and elastic nanoindentation depth

Sample	ht	hp	hp/ht	he	he/ht
	[um]	[um]	%	[um]	%
ABS	15.00 ± 0.40	8.38 ± 0.34	0.56	6.62 ± 0.20	0.44
ABS 30% Cpaint	13.64 ± 0.40	8.23 ± 0.50	0.60	5.41 ± 0.17	0.40
ABS/ CB 30% Filament	12.67 ± 0.29	8.39 ± 0.19	0.66	4.28 ± 0.18	0.34
ABS/ CB 30% Printed	5.91 ± 0.56	3.00 ± 0.44	0.51	2.91 ± 0.37	0.49
ABS/CB15% Filament	11.94 ± 0.54	7.29 ± 0.63	0.61	4.66 ± 0.23	0.39
ABS/2%CNTs/CB15% Filament	13.46 ± 0.45	8.30 ± 0.26	0.62	5.16 ± 0.25	0.38
ABS/2%CNTs/CB15% Printed	5.93 ± 0.11	3.37 ± 0.11	0.57	2.57 ± 0.03	0.43

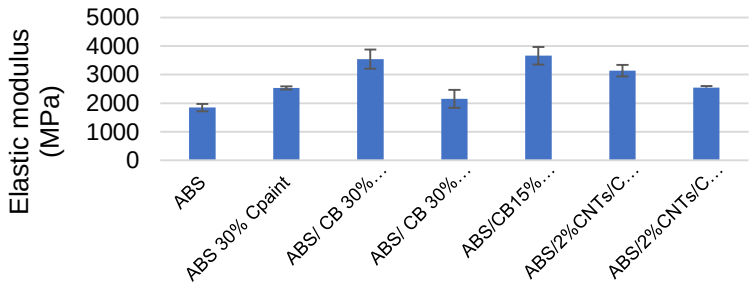

(a)

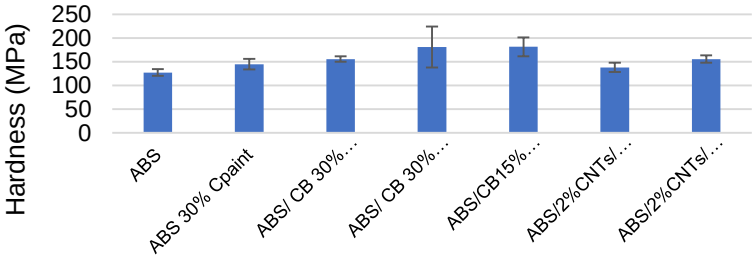

(b)

Fig. 2 Bar charts of hardness and elastic modulus of the ABS control samples and composite conductive specimens

Table 2 Hardness and elastic moduli of the materials under study

Sample	Elastic Modulus [MPa]		Hardness [MPa]	
	Average	Std. Dev.	Average	Std. Dev.
ABS	1847	130.10	127.26	6.85
ABS 30% Cpaint	2535	56.68	144.86	10.86
ABS/ CB 30% Filament	3540	335.88	155.61	5.74
ABS/ CB 30% Printed	2157	314.10	180.94	42.97
ABS/CB15% Filament	3660	309.18	181.42	19.94
ABS/2%CNTs/CB15% Filament	3138	199.91	137.96	9.68
ABS/2%CNTs/CB15% Printed	2550	49.01	155.57	7.80

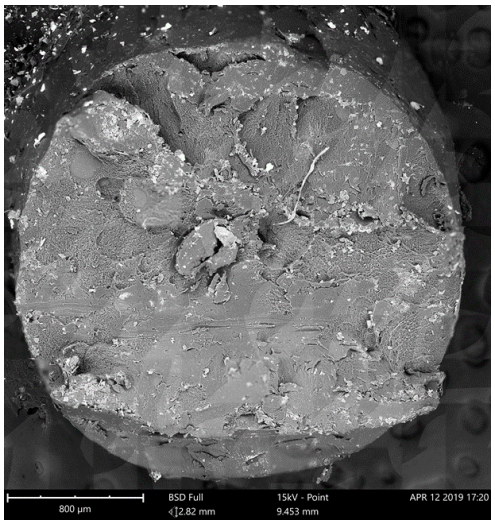

(a)

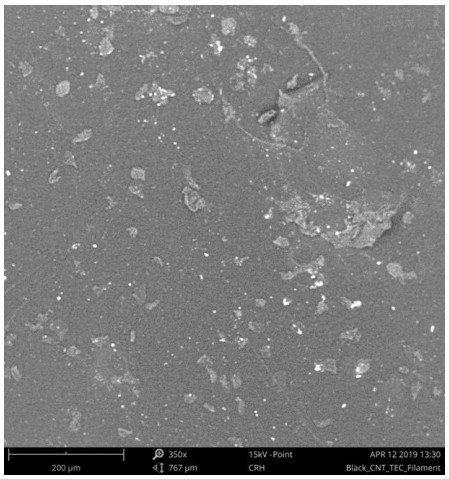

(b)

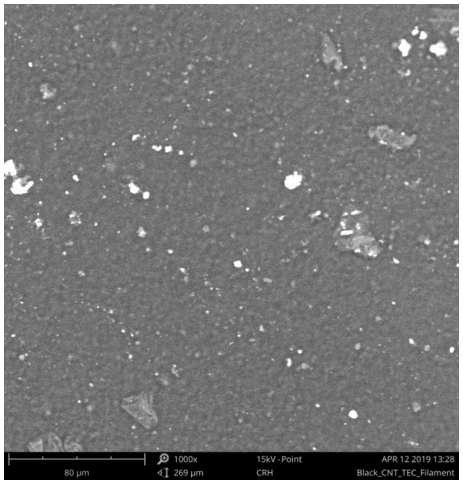

(c)

Fig. 3 (a) Cross section image of the filament, (b) sample in (500x) and (c) in higher magnification (1000x)

The These results were expected since adding carbon black fillers in ABS matrix increases the hardness of the composite as reported elsewhere (Längauer et al, 2014). Other works (Mansour et al, 2018, 2019, 2021), have shown similar results, where CNTs, graphene and carbon fibers have

increased the stiffness and the strength of the thermoplastic filament and the 3D printed specimen, as well. Furthermore, adding 15% of Carbon Black, 2% of CNTs and 5% of TEC plasticizer in the reference ABS sample, resulted in an increase in the elastic moduli by 69% in the filament and 38% in the 3D printed sample, while the hardness increased by 8% and 22% respectively. Considering the above results, the ABS/2%CNTs/CB15% composite is considered optimal, since it has demonstrated a superior mechanical behaviour compared to the reference samples and the other composites.Microstructure characterization

3.2 Microstructure characterization

Paper The material in filament form with 78% ABS, 15% Carbon Black, 2% CNTs and 5% TEC plasticizer was analyzed in a scanning electron microscope. Both the surface of the filament and the cross-section were analyzed. Figure 3 shows the absence of extensive agglomerations indicating a rather homogenous distribution of carbon black and nanotubes in ABS matrix. This means that the adopted production process, consisting of embedding CNTs and Carbon Black using the solution mixing method was capable to properly disperse CNTs and Carbon Black in the ABS matrix. The good dispersion results were expected since embedding CNTs in an acetone mixture leads to good dispersion, as reported elsewhere (Fukahori 2004). CNTs and Carbon Black are well-mixed in the ABS matrix and there is also absence of voids on the surface of the polymer. Moreover, the good dispersion between the Carbon Black and CNTs in the ABS matrix indicates that the created nanocomposite justifies the improved mechanical properties.

4 CASE STUDY: 3D PRINTED EMERGENCY STOP BUTTON

The main purpose of this section is to create a structural part that needs conductive filament to be 3D printed in order to function properly. An emergency stop (e-stop), also known as a kill switch and as an emergency power off (EPO), is called a safety mechanism widely used to shut off the majority of heavy machinery in case of an emergency, when it is impossible or time sensitive to shut down the machinery with the usual process (Guoxing, 2010). In contrast to the normal shut down process or the shut-down switch, which shuts down all the systems with a predefined order and turns off the machine without causing any damage, the emergency stop button is specifically designed to instantly abort the on-going operation (even if damage to the machine occurs) but also to be operated quickly, efficiently and simply (so that even in dangerous situations of extreme panic an operator with no particular training or even a simple by-stander can instantly activate the switch). E-Stop Buttons are mainly designed to be easily noticed, even to a random bystander.

Most e-stop buttons are equipped with a security feature, a removable, protective security barrier against any activation by accident (e.g. a simple plastic or glass cover that must be broken or lifted in order for the operator or bystander to activate it). The design of e-stop buttons is of highest importance. Therefore, kill switches are always integrated in every industrial-level machinery in order to prevent workplace injuries and deaths (Griffis 2004). Regarding international standards, the emergency stop function must be activated by an instant human action using an actuated control device that is manually activated. To reset the electrical system, the release of the E-Stop that was previously activated is a prerequisite. It should be clear that restarting the machinery is not done through resetting the E-Stop switch, that only makes it possible, but restarting the machine must be done through prerequisite procedures appropriate for each machinery. The International Electrotechnical Commission (IEC 60947-5-5, 2016) & ISO 13-850 defines the specifications of emergency stop buttons in terms of ergonomics, electrical and mechanical requirements (Fukui et al, 2007). The E-Stop button is a highly distinctive push button or "mushroom type" button, in which mechanical action with mechanical latching must be used. All electrical contacts open instantly and permanently at exactly the time the E-Stop button is pushed (activation of the protocol) through a latching mechanism. The restart of the machinery is once more able when all the electrical contacts close, for this to occur a manual key release or a twist is required for the E-Stop actuator to be unlatched.

In terms of operation, e-stop buttons use the NC (normally closed) protocol instead of no (normally open). Normally Open state is when an electrical switch contact remains open until a predetermined threshold has been reached, after that the switch closes, in order to allow the electric current flow. Normally Closed state is when an electrical switch contact remains closed until a predetermined threshold has been reached, after that the switch opens, in order to disable the electric current. The Normally Closed circuit protocol is the key characteristic of the designed kill switch.

The whole design was created with the intension of 3D printing it with a simple Fused Filament Fabrication (FFF) desktop printer (in the current

case the BCN3D Sigma Dual Extruder R17). Heavily influenced by many emergency stop button designs, a more circular e-stop was created. It consists of two main parts, each one comprised of many subparts. In the first part, a tube shape design was adopted to house the actual emergency button. On the base of the tube-shaped housing, a small circular pin was created in order to secure the spring needed to create the button effect. Two holes were added on the side of the tube opposite to each other, to house the cables from the individual circuits that will be integrated. Furthermore, two slopes opposite to each other were added on the side of the base design as guidelines of the button's movement. The slopes lead to a square hole on each side, which act as a locking mechanism to secure the button when pressed. Progressing to the second part of the design, a cylinder was created to match the tube-shaped housing. The cylinder part consists of four subparts.

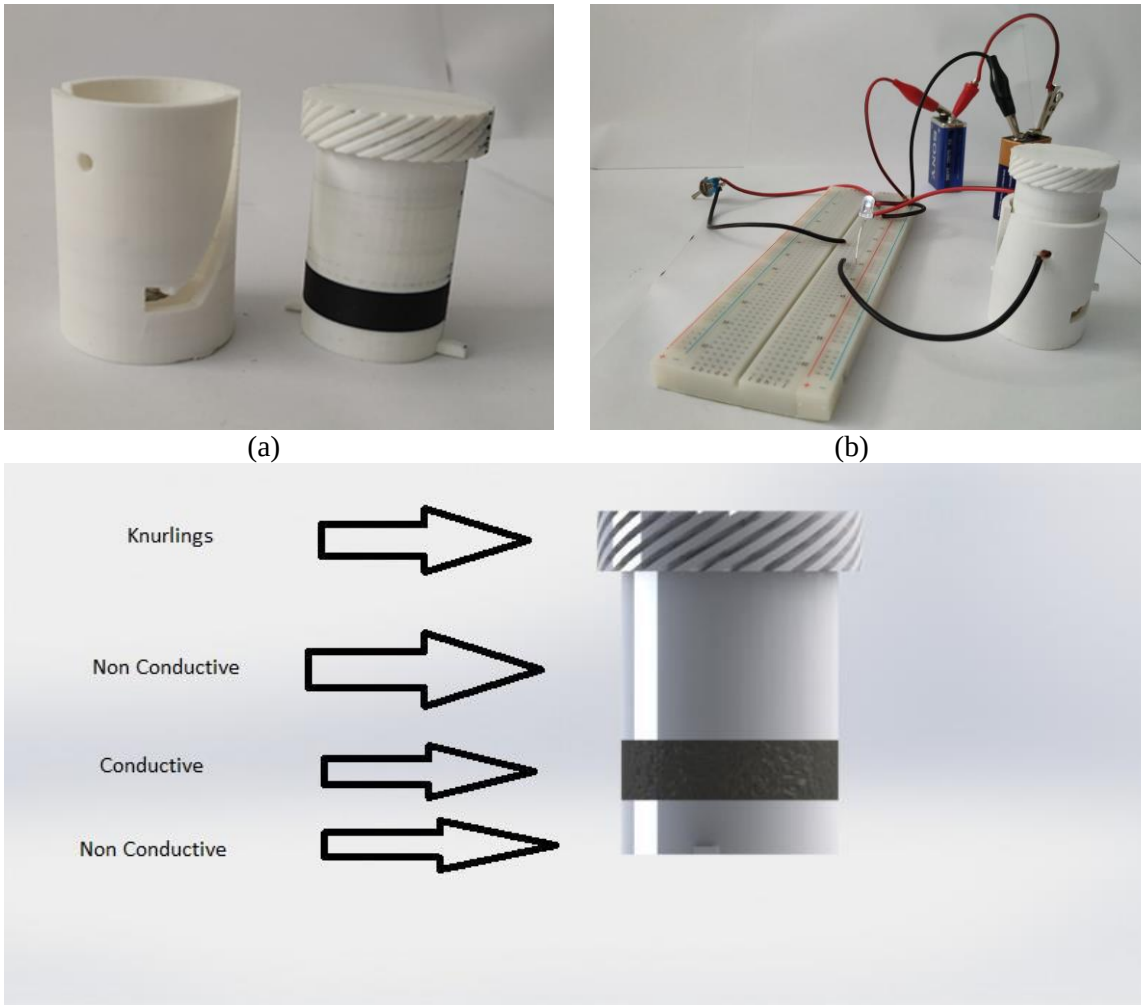

(a) (b)

(c)

Fig. 4 3D Printed Emergency Stop Button: (a) individual components of the e-stop button, (b) Complete circuit design with the individuals components of the e-stop button, (c) Activation of the emergency button design

The conductive part was placed in the middle in order to remain in contact with the cables in the normal position (not pushed). From each side nonconductive parts are placed to break the connection each time the button is pushed. On the upper part knurlings were added to help the pull and turn action (Pull and turn, in order to deactivate it and return to the original Normally Closed state. On the bottom part of the button two small pieces opposite to each other were placed to complete the locking mechanism. The complete design of the button part is shown in Figure 4.A small circuit consists of a raster board, along with a LED light and two 9V batteries as well as the prototype emergency button was created. The e-stop prototype was connected in series with the other components in order to analyze the functionality of the design. By assembling the components and powering the circuit when the emergency stop button is on the original state (normally closed position), the LED light is activated. Furthermore, on the activation of the emergency button the Led light is instantly

deactivated. The LED light does not change the off state until the e-stop button is fully deactivated (in the original state). These actions are proof that the e-stop prototype is a fully functional kill switch. The activation and deactivation states are presented in the pictures below. The 3D Printed prototype worked according to the e-stop button standards. Moreover, the response time of the produced button was equal to a usual manufactured e-stop button. Results that verify not only the conductivity of the formulated material, but also the capability of embedding the material into real-life products

5 CONCLUSIONS

This work describes the preparation, characterization and testing of conductive ABS-based thermoplastic composites suitable for electrical circuit printing using FFF-based 3D printing. Overall, it is exhibited that 3D Printing technology along with capable, efficient materials is able to manufacture functional components, incorporating electronics that can be used in simple or complex circuits, instead of being just a technology for fabricating prototypes, architectural, non-functional structures. This advancement has many possibilities for a number of fields and applications. This material offers individuals the ability to produce complex products incorporating electronic components on a low-cost, desktop printer without the need for vast production facilities.

The conductive filament was produced by using ABS as polymeric matrix in 78% combined with 15% Carbon Black along with 2% CNTs as the conductive filler and 5% TEC as plasticizer. By conducting dynamic ultra-micro-hardness tests, as well as SEM analysis, the structure along with the mechanical properties of the developed composite are defined. The formulated material has demonstrated superior mechanical properties and enabled the rapid production of functional electronic component using a simple, low-cost 3D printer. The demonstrated 3D Printed emergency stop button illustrate the potential use of this material for circuit applications.

6 REFERENCES

Assael, M.J., Antoniadis, K.D., Metaxa, I.N., Tzetzis, D., (2009) *Measurements on the enhancement of the thermal conductivity of an epoxy resin when reinforced with glass fiber and carbon multiwalled nanotubes* Journal of Chemical and Engineering Data, 2009, 54(9), pp. 2365–2370

Cephas, M., (2014). *The Impact and Application of 3D Printing Technology*. International Journal of Science and Research (IJSR).

Fukahori, Y., (2004). *Carbon Black Reinforcement of Rubber (1): General Rules of Reinforcement*. International Polymer Science and Technology. 31. 11-17. 10.1177/0307174X0403100803.

Fukui, T., Yasui, T., Obata, N., Fujimoto, M., Matsumoto, A., Fujita, T., (2007). *Development of safety technology to ensure safety of two or more operators in hazardous areas by preventing erroneous resetting*. In: International Conference-Safety of Industrial Automated Systems (SIAS 2007).

Griffis, M., *Programmable emergency-stop circuit with testing*. U.S. Patent No 6,734,581, 2004

Guoxing S., Zhengping L., Guangming, C., (2010). *Dispersion of Pristine Multi-Walled Carbon Nanotubes in Common Organic Solvents*. Nano. 5. 103-109. 10.1142/s1793292010001986.

Halidi, M., Amalina, S.,N., Abdullah, J., (2012). *Moisture and Humidity Effects on the ABS Used in Fused Deposition Modeling Machine*. Advanced Materials Research. 576. 641-644.

Horst, D., Júnior, P., (2019). *3D-Printed Conductive Filaments Based on Carbon Nanostructures Embedded in a Polymer Matrix: A Review*. International Journal of Applied Nanotechnology Research. 4. 10.4018/IJANR.2019010103.

Klonos, P.A., Papadopoulos, L., Tzetzis, D., Kyritsis, A., Papageorgiou, G.Z., Bikiaris, D.N., (2019) *Thermal, nanoindentation and dielectric study of nanocomposites based on poly(propylene furanoate) and various inclusions.* Materials Today Communications, 2019, 20, 100585

Längauer, M., Liu, K., Kneidinger, C., Schaffler, G., Purgleitner, B., Zitzenbacher, G., (2014). *Experimental analysis of the influence of pellet shape on single screw extrusion*. Journal of Applied Polymer Science. 132. 10.1002/app.41716.

Mansour, G., Tzetzis, D., Bouzakis, K.D., (2013) *A nanomechanical approach on the measurement of the elastic properties of epoxy reinforced carbon nanotube nanocomposites*. Tribology in Industry, 2013, 35(3), pp. 190–199

Mansour, G., Tzetzis, D., (2013) *Nanomechanical Characterization of Hybrid Multiwall Carbon Nanotube and Fumed Silica Epoxy Nanocomposites*. Polymer - Plastics Technology and Engineering, 2013, 52(10), pp. 1054–1062

Mansour, G., Tsongas, K., Tzetzis, D., Tzikas, K., (2017) *Dynamic mechanical characterization of polyurethane/multi-walled carbon nanotube composite thermoplastic elastomers*. Polymer-Plastics Technology and Engineering; 56(14):1505-

1515. https://doi.org/10.1080/03602559.2016.1277243

Mansour G., Zoumaki M., Tsongas K., Tzetzis D., (2021) *Microstructural and Finite Element Analysis-assisted Nanomechanical Characterization of Maize Starch Nanocomposite Films*. Materials Research 2021; 24(2): e20200409. https://doi.org/10.1590/1980-5373-mr-2020-0409

Mansour, M., Tsongas, K., Tzetzis, D., Antoniadis, A., (2018) *Mechanical and Dynamic Behavior of Fused Filament Fabrication 3D Printed Polyethylene Terephthalate Glycol Reinforced with Carbon Fibers*. Polymer - Plastics Technology and Engineering, 2018, 57(16), pp. 1715–1725

Mansour, M., Tsongas, K., Tzetzis, D., (2019) *Measurement of the mechanical and dynamic properties of 3D printed polylactic acid reinforced with graphene*. Polymer-Plastics Technology and Materials, 2019, 58(11), pp. 1234–1244

Mansour M.T., Tsongas K., Tzetzis D., (2021) *3D Printed Hierarchical Honeycombs with Carbon Fiber and Carbon Nanotube Reinforced Acrylonitrile Butadiene Styrene*. Journal of Composites Science. 2021; 5(2):62. https://doi.org/10.3390/jcs5020062

Marasso, S., Cocuzza, M., Bertana, V., Perrucci, F., Tommasi, A., Ferrero, S., Scaltrito, L., Pirri, C., (2018). *PLA conductive filament for 3D printed smart sensing applications*. Rapid Prototyping Journal. 24. 00-00. 10.1108/RPJ-09-2016-0150.

Moore, J.D., (1973). *Acrylonitrile-butadiene-styrene (ABS) - a review*, Composites, Volume 4, Issue 3

Novotny, V., & Bryksí S., B., Schastlivtseva, E., Zikmund, P., (2018). *3D Printed Parts for Power Industry*.

Oliver, W., Pharr, G., (1992) *An improved technique for determining hardness and elastic modulus using load and displacement sensing indentation experiments*. Journal of Materials Research 7(6):1564-1583. https://doi.org/10.1557/JMR.1992.1564

Suder, P., Novák, P., Havlíček, V., Bodzoń-Kułakowska, A., (2016). *General Strategies for Proteomic Sample Preparation*, Editor(s): P. Ciborowski, J. Silberring, *Proteomic Profiling and Analytical Chemistry* (Second Edition), Elsevier

Teanmetawong, S., Chantaramanee, T., Lhosupasirirat, S., Wongariyakawee, A., Srikhirinet T., (2019), *A Comparison Study of Magnetic Stirrer and Sonicator Technique to Disperse 1% Span20 Treated Layered Double Hydroxides (LDHs)* IOP Conf. Ser.: Mater. Sci. Eng. 654 01200510.4028/www.scientific.net/AMR.576.641.

Tsongas, K., Tzetzis, D., Mansour, G., (2017) *Mechanical and vibration isolation behaviour of acrylonitrile-butadiene rubber/multi-walled carbon nanotube composite machine mounts*. Plastics, Rubber and Composites, 2017; 46(10):458-468. http://dx.doi.org/10.1080/14658011.2017.1391975

Tsongas, K., Tzetzis, D., Karantzalis, A.E., Banias G., Ahmadkhaniha, D., Zanella, C., Matikas, T.E., Bochtis, D., (2019). *Microstructural, Surface Topology and Nanomechanical Characterization of Electrodeposited Ni-P/SiC Nanocomposite Coatings*, Vol. 9, 2901

Tzetzis, D., Tsongas, K., Mansour G., (2017) *Determination of the Mechanical Properties of Epoxy Silica Nanocomposites through FEA-Supported Evaluation of Ball Indentation Test Results*, Materials Research, vol.20 (6), pp.1571-1578

Vieira, M., G., A., Altenhofen da Silva, M., Oliveira dos Santos, L., Beppu, M., M., (2011) *Natural-based plasticizers and biopolymer films: A review*, European Polymer Journal, Volume 47, Issue 3

Wei, X., Li, D., Jiang, W., Gu, Z., Wang, X., Zhang, Z., Sun, Z., (2015). *3D Printable Graphene Composite*. Scientific reports. 5. 11181. 10.1038/srep11181.